ADVANCES IN ATMOSPHERIC SCIENCES, VOL. 31, MAY 2014, 505–514

Development of the IAP Dynamic Global Vegetation Model

ZENG Xiaodong*, LI Fang, and SONG Xiang

International Center for Climate and Environmental Sciences, Institute of Atmospheric Physics, Chinese Academy of Sciences, Beijing 100029

(Received 24 July 2013; revised 28 August 2013; accepted 30 August 2013)

ABSTRACT

The IAP Dynamic Global Vegetation Model (IAP-DGVM) has been developed to simulate the distribution and structure of global vegetation within the framework of Earth System Models. It incorporates our group's recent developments of major model components such as the shrub sub-model, establishment and competition parameterization schemes, and a process-based fire parameterization of intermediate complexity. The model has 12 plant functional types, including seven tree, two shrub, and three grass types, plus bare soil. Different PFTs are allowed to coexist within a grid cell, and their state variables are updated by various governing equations describing vegetation processes from fine-scale biogeophysics and biogeochemistry, to individual and population dynamics, to large-scale biogeography. Environmental disturbance due to fire not only affects regional vegetation competition, but also influences atmospheric chemistry and aerosol emissions. Simulations under observed atmospheric conditions showed that the model can correctly reproduce the global distribution of trees, shrubs, grasses, and bare soil. The simulated global dominant vegetation types reproduce the transition from forest to grassland (savanna) in the tropical region, and from forest to shrubland in the boreal region, but overestimate the region of temperate forest.

Key words: Dynamic Global Vegetation Model, individual and population dynamics, biogeography, disturbance

Citation: Zeng, X. D., F. Li, and X. Song, 2014: Development of the IAP Dynamic Global Vegetation Model. *Adv. Atmos. Sci.*, **31**(3), 505–514, doi: 10.1007/s00376-013-3155-3.

1. Introduction

About two thirds of the Earth's land surface is covered by vegetation, characterizing the interface between land and atmosphere interactions. It is well known that natural vegetation is influenced mainly by climate (e.g., Box, 1981; Lugo et al., 1999; Ricklefs, 2008), and ecosystem state is usually a response to gradual, smooth and continuous climate change, but may change abruptly as climate conditions approach a critical threshold, irreversibly switching to a contrasting state (Scheffer et al., 2001, 2009). This latter situation has been observed over history (e.g., the collapse of vegetation in the Sahara around 5000 years ago) (Lenton et al., 2008), and currently the threat of forest dieback in Amazonia (Nobre and Borma, 2009; Davidson et al., 2012) and boreal regions (Lenton et al., 2008) over the next 100 years is of great concern. Dramatic changes in ecosystem state may in turn reinforce the trend of climate change (Lenton, 2011) through regulating the energy, water, and carbon exchanges between land and atmosphere.

As part of recognizing the important roles of the terrestrial ecosystem in global climate and environment change studies, various Dynamic Global Vegetation Models (DGVMs) have been developed in the last 20 years (Foley et al., 1996; Friend et al., 1997; Potter and Klooster, 1999; Woodward et al., 2000; Cox, 2001; Moorcroft et al., 2001; Sitch et al., 2003; Levis et al., 2004; Sato et al., 2007), and become one of the key components of dynamic Earth System Models (ESMs). DGVMs mostly apply mechanistic parameterizations of large-scale vegetation processes (i.e., individual and population dynamics, disturbance) (Prentice et al., 2007) to simulate the distribution and structure of global vegetation, as well as its evolution, alongside global climate change. They provide surface information on large-scale vegetation states, as well as carbon emissions released by soil heterotrophic respiration and wild fires, required by land and atmospheric models.

IAP-DGVM is a DGVM developed at the Institute of Atmospheric Physics, Chinese Academy of Sciences. Its purpose is to address the following disadvantages of current DGVMs: (1) Although DGVMs are capable of capturing the major regions of trees and grasses, their performances in semiarid regions are usually less accurate and several DGVMs replace shrub with grass and bare soil (e.g., Sitch et al., 2003; Levis et al., 2004); (2) The ecological processes of population dynamics (e.g., establishment) in many DGVMs are oversimplified, leading to various inconsistent behaviors (Song, 2012; Song and Zeng, 2014); (3) Regardless of the differences in the complexities of fire parameterization

* Corresponding author: ZENG Xiaodong
Email: xdzeng@mail.iap.ac.cn

schemes used in DGVMs, large biases exist in the simulation of global fire burned area and carbon emissions (Li et al., 2012a).

The paper is organized as follows. The structure of the model, including the biogeography and population dynamics, individual dynamics, biogeophysics and biogeochemistry, and disturbance (fire), is presented in detail in section 2. A brief demonstration of the model's performance is reported in section 3. And finally, a summary and further discussion is provided in section 4.

2. Model description

2.1. *Overview*

IAP-DGVM adopts concepts from the Lund–Potsdam–Jena (LPJ) Dynamic Global Vegetation Model (Sitch et al., 2003) and the Community Land Model's Dynamic Global Vegetation Model (CLM-DGVM) (Levis et al., 2004), but also incorporates our recent developments of major model components such as the shrub sub-model (Zeng et al., 2008; Zeng, 2010), establishment and competition parameterization schemes (Song, 2012; Song and Zeng, 2014), a process-based fire parameterization of intermediate complexity (Li et al., 2012a, 2012b), as well as some other modifications.

In DGVMs, plants are usually classified into plant functional types (PFTs) according to their physical, phylogenetic and phenological characteristics. IAP-DGVM uses 12 PFTs (Table 1), including seven tree, two shrub, and three grass types, plus bare soil. The model applies the mean field theory in representing the local ecosystem structure. While all PFTs are allowed to coexist in a grid cell (or vegetated land area), each PFT is assumed to have homogeneous spatial distribution, and is represented by a group of so-called average individuals, i.e., the differences among individuals within each PFT are neglected. Each woody PFT (tree or shrub) is assigned a set of prognostic variables of the population and individual states, with the former including population density of woody vegetation (i.e., number of individuals per unit land area), P, and the latter mainly consisting of the carbon pools of leaf, root, sapwood and heartwood per individual, i.e., $C_{\rm l}$, $C_{\rm r}$, $C_{\rm sw}$, and $C_{\rm hw}$, respectively (units: g carbon per individual). Because it is difficult to distinguish the individuals of grass in the model, grass PFTs are always virtually assigned a population density of $P = 1$, and the units of $C_{\rm l}$ and $C_{\rm r}$ are g carbon per unit area of grid cell (grass PFTs do not have carbon pools of sapwood and heartwood).

While the state variables are updated by various governing equations, the ecosystem large-scale properties, such as PFT fractional coverage (FC) and leaf area index (LAI), which are inferred from the state variables, are also provided in order to facilitate coupling with other components in the ESM. To be consistent with most Land Surface Models (LSMs), which do not allow the overlap of vegetation canopies, the total FCs of all PFTs in a grid cell cannot exceed 100% (see section 2.2.3, below), and the area not covered by vegetation is set to be bare soil.

According to the spatial and temporal scales of the involved ecological processes, IAP-DGVM can be categorized into four sub-modules (Fig. 1).

2.2. *Biogeography and population dynamics*

2.2.1. *Biogeography*

The biogeography, describing the climatic constraints of survival and establishment (see Table 1), is similar to CLM-DGVM. PFT survival in a grid cell requires the long-term average (e.g., 20-yr running mean) of the minimum monthly temperature, $T_{\rm c}$, to exceed $T_{\rm c,min}$. Existing PFTs cease to exist if they cannot survive. Besides, PFTs will also be removed if their annual net primary production (NPP) is negative.

In addition to the above criteria, establishment also requires $T_{\rm c}$ to be less than $T_{\rm c,max}$, $\rm GDD_5$ to be greater than $\rm GDD_{min}$, $\rm GDD_{23}$ to be equal to 0, and annual precipitation

Table 1. List of PFTs and their bioclimatic constraints of survival and establishment.

PFT	Survival	Establishment	
	$T_{\rm c,min}$ (°C)	$T_{\rm c,max}$ (°C)	$\rm GDD_{min}$
Trees			
Broadleaf Evergreen Tropical	15.5	-	0
Broadleaf Deciduous Tropical	15.5	-	0
Broadleaf Evergreen Temperate	3.0	18.8	1200
Needleleaf Evergreen Temperate	−2.0	22.0	900
Broadleaf Deciduous Temperate	−17.0	15.5	1200
Needleleaf Evergreen Boreal	−32.5	−2.0	600
Broadleaf Deciduous Boreal	-	−2.0	350
Shrubs			
Broadleaf Deciduous Temperate	−17.0	-	1200
Broadleaf Deciduous Boreal	-	−2.0	350
Grasses			
C4	15.5	-	0
C3 Non-arctic	−17.0	15.5	0
C3 Arctic	-	−17.0	0

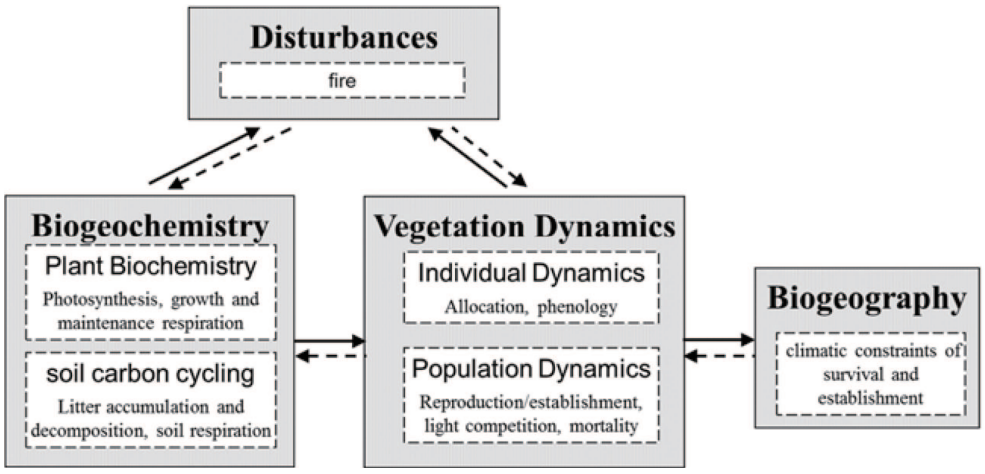

Fig. 1. Components of IAP-DGVM showing the four sub-modules and the major ecological processes involved.

to be greater than 100 mm yr^{-1}, where GDD_5 and GDD_{23} are the long-term averages of the annual growing degree days above 5°C and 23°C respectively, and $T_{c,min}$, $T_{c,max}$, and GDD_{min} are PFT-dependent constants.

The dynamics of population density of the ith woody PFT, P_i, is determined by

$$\begin{aligned} P_i(t+1) &= P_i(t) + \Delta P_i \ , \\ \Delta P_i &= \Delta P_{\mathrm{est},i} - \Delta P_{\mathrm{m},i} \ , \\ \Delta P_{\mathrm{m},i} &= \Delta P_{\mathrm{light},i} + \Delta P_{\mathrm{sg},i} + \Delta P_{\mathrm{fire},i} \ , \end{aligned} \tag{1}$$

where $P(t)$ and $P(t+1)$ are the population densities at the current and next time step; ΔP is the change in population density; ΔP_{est} is the population increase due to establishment; and ΔP_{m} is population decrease due to mortalities, including $\Delta P_{\mathrm{light}}$, ΔP_{sg}, ΔP_{sh}, and ΔP_{fire}, which are caused by light competition, growth stress, heat stress, and fire, respectively. Except for ΔP_{fire}, which will be described in section 2.5, the other terms are summarized as follows.

2.2.2. *Establishment*

In DGVMs, establishment of woody vegetation refers to a sequence of reproduction and regeneration processes from flowering, fertilization, seed production, germination, and finally growth of saplings. IAP-DGVM applies a hierarchy of tree–grass–shrub for the competition of establishment. Trees can establish in areas currently not occupied by perennial vegetation, i.e., trees and shrubs. The establishment rate of a given tree PFT is calculated once a year as:

$$\begin{aligned} \Delta P_{\mathrm{est},i} &= \Delta P_{\mathrm{est,tree}} \frac{g_i}{\sum_{k=1}^{n_{\mathrm{est,tree}}} g_k} e^{-\gamma \cdot \mathrm{FC_{tree}}} (1 - m_i) \ , \\ \Delta P_{\mathrm{est,tree}} &= \Delta P_{\mathrm{estmax,tree}} (1 - \mathrm{FC_w}) [1 - e^{-5(1-\mathrm{FC_w})}] \ , \\ g_i &= g_{i0} [\varepsilon_0 + (1 - \varepsilon_0) \mathrm{FC}_i^{\sigma}] \ , \\ m_i &= e^{-\alpha m_{\mathrm{ge},i} + \beta m_{\mathrm{heat},i}} \ , \end{aligned} \tag{2}$$

where $\Delta P_{\mathrm{est,tree}}$ is the total establishment rate of tree PFTs in the grid cell; $n_{\mathrm{est,tree}}$ is the number of tree PFTs established in the current time-step; $\Delta P_{\mathrm{estmax,tree}}$ is a constant representing the maximum establishment rate of trees; $\mathrm{FC_w}$ is the total coverage of trees and shrubs in the grid cell; the term $(1 - \mathrm{FC_w})$ is the area currently not covered by trees, and so available for establishment; the term $1 - e^{-5(1-\mathrm{FC_w})}$ refers to the shading effects (Sitch et al., 2003); g_i represents the competition of establishment among different woody PFTs, including the establishment from seeds produced in the current year, which is assumed to be dependent on PFT FC, FC_i, with an exponential factor, σ as well as background establishment ε (i.e., from seeds produced in previous years or propagated from nearby grid cells); g_{i0} is the PFT-dependent constant of relative establishment potential which represents the competition–colonization trade-off among different PFTs (Song, 2012; Song and Zeng, 2014); and m_i is the mortality rate of seedlings, inferred from the individual background mortality, m_{ge}, and mortality due to heat stress, m_{heat} [Eqs. (7) and (8)]

Grasses and shrubs can establish only in bare soil. IAP-DGVM does not consider the shading effects on grass establishment, and young grass seedlings are added over all bare areas in proportion to the current FC of different grass PFTs, i.e.,

$$\begin{aligned} \Delta \mathrm{FC}_{\mathrm{est},i} &= (1 - \mathrm{FC_{veg}}) \frac{g_i}{\sum_{k=1}^{n_{\mathrm{est,tree}}} g_k} \ , \\ g_i &= g_{i0} [\varepsilon_0 + (1 - \varepsilon_0) \mathrm{FC}_i] \ , \end{aligned} \tag{3}$$

where $\mathrm{FC_{veg}}$ is total vegetation coverage of the grid cell; $n_{\mathrm{est,grass}}$ is the number of grass PFTs established in the current time-step; and g_i, g_{i0}, and ε_0 are the same as in tree establishment.

Establishment of shrub PFTs follows the same rule as trees, i.e., Eq. (2), but replace the term $\Delta P_{\mathrm{estmax,tree}}$ with $\Delta P_{\mathrm{estmax,shrub}}$, and $\mathrm{FC_w}$ with $\mathrm{FC_{veg}}$.

2.2.3. *Light competition*

In IAP-DGVM, light competition occurs if the total FCs of specific vegetation categories exceed corresponding thresholds. The model applies a hierarchy of tree–shrub–grass for the light competition to represent the advantage of higher vegetation in capturing incoming solar radiation. First, if the total tree coverage in a grid cell, $\mathrm{FC_{tree}}$, is larger than

a threshold (95% in the model), the excess is removed from existing tree PFTs in proportion to their FCs through the decrease of population densities (Sitch et al., 2003). Thus, the mortality due to light competition is calculated as

$$\Delta P_{\mathrm{light},i} = \left(1 - \frac{0.95}{\mathrm{FC_{tree}}}\right) P_i \ . \tag{4}$$

Shrubs are usually shorter than trees but taller than grasses; hence, shrubs can occupy the area not covered by trees. Because there are only two shrub PFTs and they cannot coexist in the same grid cell, the excess cover when total tree and shrub coverage, $\mathrm{FC_w}$, is larger than 100% is removed by the only existing shrub in the grid cell, i.e.,

$$\Delta P_{\mathrm{light},i} = \left(\frac{\mathrm{FC_w} - 1.0}{\mathrm{FC}_i}\right) P_i \ . \tag{5}$$

Finally, grasses may occur only in areas not covered by woody vegetation. The excess cover is removed by directly reducing the FC of grass PFTs:

$$\Delta \mathrm{FC}_{\mathrm{light},i} = \frac{\mathrm{FC_{veg}} - 1.0}{\mathrm{FC_{grass}}} \mathrm{FC}_i \ . \tag{6}$$

2.2.4. *Mortality due to growth stress*

It has been observed that individuals with relatively lower growth rates usually have higher mortality rates (Bugmann, 2001; Keane et al., 2001). Following Prentice et al. (1993), the related mortality rate, $m_{\mathrm{ge},i}$, is inversely related to the growth efficiency (ge_i), which is defined as the ratio of net biomass increment per individual, ΔC_i, to individual leaf area:

$$\begin{aligned} \Delta P_{\mathrm{sg},i} &= m_{\mathrm{ge},i} P_i \ , \\ m_{\mathrm{ge},i} &= \frac{k_{\mathrm{m1}}}{1 + k_{m2}\mathrm{ge}_i} \ , \\ \mathrm{ge}_i &= \frac{\Delta C_i}{C_{l,i}\mathrm{SLA}} \ , \end{aligned} \tag{7}$$

where SLA is the specific leaf area (leaf area per unit leaf mass); PFT-dependent k_{m1} is the corresponding maximum mortality rate, i.e., the mortality rate as $\mathrm{ge} = 0$; and k_{m2} is a constant.

2.2.5. *Mortality due to heat stress*

It has been noticed that high temperatures can cause tissue damage to temperate and boreal vegetation, and even result in losses of individuals. The related mortality rate is calculated as

$$\begin{aligned} \Delta P_{\mathrm{sh},i} &= m_{\mathrm{heat},i} P_i \ , \\ m_{\mathrm{heat},i} &= \frac{\mathrm{GDD_{23}}}{300} \ , \end{aligned} \tag{8}$$

where $\mathrm{GDD_{23}}$ is the averaged annual growing degree days above 23°C (see section 2.2.1).

2.2.6. *Changes in average individual carbon pools*

Because IAP-DGVM does not consider the dynamics of seedling and mature individuals separately, the individual carbon pools are updated by averaging the remaining individuals and the newly established saplings. For woody PFTs, it is

$$C_{\mathrm{tis},i}(t+1) = \frac{C_{\mathrm{tis},i}(t)(P_i(t) - \Delta P_{\mathrm{m},i}) + C_{\mathrm{tis,sap},i}\Delta P_{\mathrm{est},i}}{P_i(t+1)} \ , \tag{9}$$

where subscript "tis" stands for leaf, root, sapwood, or heartwood; and C_{sap} are the pre-described sapling carbon pools.

For grass,

$$C_{\mathrm{tis},i}(t+1) = C_{\mathrm{tis},i}(t) + C_{\mathrm{tis,sap},i}\Delta \mathrm{FC}_{\mathrm{est},i} \ . \tag{10}$$

2.3. *Individual dynamics*

The processes of individuals include the allocation of NPP to different tissues, tissue turnover, and the seasonal variation of leaf area, i.e., leaf phenology.

2.3.1. *Allocation and plant morphology*

Annual NPP, i.e., photosynthesis minus plant respiration (see section 2.4), is allocated to reproduction (for establishment) and different tissue carbon pools (for individual growth). While the fraction of reproduction costs could be PFT-dependent and be related to the relative establishment potential, g_{i0} [see Eq. (2)] it is set to a fixed 10% with $g_{i0} \equiv 1$ for simplification in the current model.

The allocation to leaves, sapwood, and roots of woody vegetation is calculated so that the individual carbon pools follow the allometric relationships modified from Sitch et al., (2003) and Levis et al. (2004):

$$\begin{aligned} a_{\mathrm{l}} &= k_{\mathrm{1s}} a_{\mathrm{s}} \ , \\ C_1 &= k_{\mathrm{1r}} C_{\mathrm{r}} \ , \\ H &= k_{a2} \mathrm{D}^{k_{\mathrm{a3}}} \ , \\ a_{\mathrm{C}} &= k_{a1} \mathrm{D}^{k_{\mathrm{rp}}}, \quad a_{\mathrm{C}} < a_{\mathrm{C,max}} \end{aligned} \tag{11}$$

where a_{l} and a_{s} are the individual leaf area and sapwood cross-sectional area, respectively; H, D, and a_{C} stand for height, stem diameter and crown area; and the parameters k_{ls}, k_{lr}, k_{a1}, k_{a2}, k_{a3}, k_{rp}, and $a_{\mathrm{c,max}}$ are PFT-dependent (see Table 2).

Comparing the second equation of Eq. (11) with Eq. (2) of Sitch et al. (2003) and Eq. (23) of Levis et al. (2004), a factor representing the degree of water stress, ω, is removed from the right-hand side. The original purpose of introducing ω was to capture the feature that plants may have higher root-to-leaf ratios as water stress increases. However, the capacity of roots to absorb soil water for transpiration, and hence the strength of plant photosynthesis, is not related with total root biomass in most current LSMs, and the strategy of increased allocation to roots along with decreased allocation to leaves

Table 2. Parameters for woody plant morphology.

	$k_{\mathrm{la:sa}}$	k_{allom1}	k_{allom2}	α_{cmax} ($\mathrm{m^2}$)
Broadleaf trees	8000	100	40	15
Needleleaf trees	8000	82	40	15
Shrubs	4000	200	10	5

will result in higher root respiration and lower photosynthesis capacity, i.e., making the situation for plants under water stress undesirable. Hence, ω has been temporally dropped before further development in LSMs.

Besides, the k_{a1} of temperate and boreal needle-leaf evergreen trees is set to be 82, compared with 100 for other tree PFTs, to reflect the morphological feature of a relatively smaller but denser canopy. The parameters for two shrub PFTs are also defined and different to tree PFTs following Zeng (2010).

On the other hand, allocation for grass PFTs is simpler in that only the second equation in Eq. (11) is needed, because grass does not have the carbon pools for sapwood and heartwood.

2.3.2. *Turnover*

Each year, plants may lose part or all of their leaves and roots, and part of the sapwood of woody PFTs may turn into heartwood, due to turnover. The decrease in the corresponding tissue carbon pool is calculated as

$$\Delta C_{\rm tis} = f_{{\rm tis},i} C_{\rm tis} \ , \tag{12}$$

where $f_{{\rm tis},i}$ are PFT-dependent tissue turnover times ($\rm yr^{-1}$).

2.3.3. *Leaf phenology*

While the annual maximum LAI, $\rm LAI_{max}$, is determined by the individual leaf mass and crown area (see section 2.6), daily LAI, $\rm LAI_{daily}$, is a fraction of $\rm LAI_{max}$ and may have seasonal variation, calculated as

$$\rm LAI_{daily} = \varphi LAI_{max} \ , \tag{13}$$

where φ represents leaf phenology and has a value between 0 and 1.

Similar to Levis et al. (2004), tree phenology may be evergreen, summergreen, or raingreen: (1) For evergreen trees, $\varphi \equiv 1$, i.e., there is no seasonal variation; (2) For summergreen trees, leaves emerge evenly within 50 days after the day with $\rm GDD_5 > 100$, and drop at a rate of 1/15 $\rm d^{-1}$ when the 10-day running mean of surface air temperature, $T_{\rm 10d}$, is lower than the long-term average of the minimum monthly temperature; (3) For rain-green trees, leaves emerge or drop at a rate of 1/15 $\rm d^{-1}$ as the 10-day running mean of photosynthesis, $A_{\rm 10d}$, is larger or smaller than leaf maintenance respiration, $R_{\rm 10d,leaf}$. However, φ retains a minimum value, e.g., 0.1, to permit non-zero photosynthesis.

For the shrub PFTs, broadleaf deciduous temperate shrub is assigned as rain-green, and broadleaf deciduous boreal shrub as summer-green, for the tree phenology (Zeng, 2010).

Grass PFTs have no predetermined phenology, but respond to a blend of summer-green and rain-green (Levis et al., 2004). Leaves emerge at a rate of 1/5 $\rm d^{-1}$ if both criteria of $T_{\rm 10d} > 0^\circ$C and $A_{\rm 10d} > R_{\rm 10d,leaf}$ are satisfied, and otherwise drop at the same rate.

2.4. *Biogeochemistry and biogeophysics*

The microscale processes involved can be separated into two parts: (1) biogeochemical processes, which include photosynthesis, autotrophic respiration, litter decomposition and heterotrophic respiration; and (2) biogeophysical processes, which mainly include energy and water exchange between vegetation and land, and the surface and atmosphere. Because most of the related processes, especially photosynthesis and biogeophysical processes, are essential components of LSMs, we only briefly describe here the calculations related to NPP, which is needed by allocation, as well as accumulation and decomposition of aboveground litter, which may influence fire simulation.

2.4.1. *Net primary production*

Plants gain carbon through photosynthesis and lose carbon through autotrophic respiration, which can usually be separated into two parts, i.e., growth respiration and maintenance respiration. Maintenance respiration refers to metabolism occurring in an organism that is needed to maintain that organism in a healthy, living state. Following LPJ and CLM-DGVM, maintenance respiration amounts from leaves, roots, and sapwood (per unit area of PFT cover) are calculated respectively as

$$R_{1,i} = \varphi r \frac{c_1}{\rm cn_1} g(T_1) \frac{P_i}{\rm FC_i} \ , \tag{14}$$

$$R_{{\rm r},i} = \varphi r \frac{c_{\rm r}}{\rm cn_r} g(T_{\rm r}) \frac{P_i}{\rm FC_i} \ , \tag{15}$$

$$R_{{\rm sw},i} = r \frac{c_{\rm sw}}{\rm cn_{sw}} g(T_{\rm sw}) \frac{P_i}{\rm FC_i} \ , \tag{16}$$

where r is a PFT-dependent coefficient in grams of carbon per gram of nitrogen (gC g $\rm N^{-1}$); $\rm cn_l$, $\rm cn_r$, and $\rm cn_{sw}$ are tissue C:N ratios; $T_{\rm l}$, $T_{\rm r}$, and $T_{\rm sw}$ are tissue temperature; and φ is the leaf phenology (section 2.3).

Plants are able to grow only when annual photosynthesis is greater than the total maintenance respiration,

$$R_{{\rm m},i} = R_{1,i} + R_{{\rm r},i} + R_{{\rm sw},i} \ . \tag{17}$$

Part of the net carbon gain between photosynthesis and respiration is consumed as growth respiration, i.e.,

$$R_{{\rm g},i} = k_{\rm g}(A - R_{{\rm m},i}) \ , \tag{18}$$

where A is photosynthesis (per unit area of PFT cover), and $k_{\rm g}$ is a constant assumed to be 25%.

Then, the annual NPP available for allocation is

$$\rm NPP_i = A - R_{m,i} - R_{g,i} \ . \tag{19}$$

2.4.2. *Accumulation and decomposition of aboveground litter*

Plants can lose tissue due to individual mortality [Eqs. (4)–(10)], turnover [Eq. (12)], and fire [Eqs. (23)–(25)]. The corresponding leaves, sapwood and heartwood are added to the carbon pool of aboveground litter.

On the other hand, part of the aboveground litter is burned by fire, and the remaining part will decompose following first-order kinetics,

$$\frac{dC_{\rm L,ag}}{dt} = -k_{\rm dec} C_{\rm L,ag} \ . \tag{20}$$

where $k_{\rm dec}$ is the decomposition rate.

2.5. *Fire*

Fire is the primary terrestrial ecosystem disturbance agent on a global scale, and shapes not only ecosystem composition but also vegetation succession and regeneration (Bowman et al., 2009). IAP-DGVM adopts a process-based fire parameterization of intermediate complexity developed by Li et al. (2012a, 2012b). Methodologically, it has better structure, parameter estimation, and mathematical derivation than other process-based fire models of intermediate complexity (e.g., Glob-FIRM, CTEM-FIRE, and their modified versions). The fire model comprises three parts, i.e., fire occurrence, fire spread, and fire impact. In this paper, only the basic function and parameterization regarding the impact of fire on vegetation is briefly described; the detail of the model can be found in Li et al. (2012a, 2012b).

In the fire model, the burned area is determined by climate and weather conditions, vegetation composition and structure, and human activities. The basic function of the fire model is as follows:

$$A_{\rm b} = N_{\rm f} a \ , \tag{21}$$

where $A_{\rm b}$ is the burned area in a grid cell per time step [km^2 (time step)$^{-1}$]; $N_{\rm f}$ [count (time step)$^{-1}$] is fire counts in the grid cell, and is a function of the number of ignition sources due to natural causes and human activities, availability and combustibility of fuel (i.e., aboveground biomass of leaves, stems and aboveground litter combined), and fire suppression by human activities [see Eqs. (2)–(10) of Li et al. (2012a)]; and a (km^2) is the average spread area of a fire, and depends on wind speed [see Eqs. (11)–(18) of Li et al. (2012a)]. We define $k_{\rm fire}$ as the percentage of burned area in the grid cell, i.e., the ratio of burned area, $A_{\rm b}$, to the area of the grid cell, $A_{\rm g}$ (km^2):

$$k_{\rm fire} = \frac{A_{\rm b}}{A_{\rm g}} \ . \tag{22}$$

Within the burned area, a proportion of tissue (per individual) is burned (and becomes fire emission), given by

$$\Delta C_{{\rm fire,tis},i} = C_{{\rm tis},i} L_{\rm tis} \ , \tag{23}$$

where $L_{\rm tis}$ is the PFT-dependent combustion completeness factor for different tissues.

Besides, a proportion of woody individuals are directly killed by fire. The individual mortalities for woody PFTs due to fire, $\Delta P_{\rm fire,i}$, is calculated as

$$\Delta P_{{\rm fire},i} = k_{\rm fire} P_i \xi \ , \tag{24}$$

where ξ is the PFT-dependent whole-plant mortality factor. On the other hand, survival would lead to loss of part of the uncombusted tissue, and would transfer to litter. The tissue mortalities are:

$$\Delta C_{{\rm m,tis},i} = C_{{\rm tis},i}(1 - L_{\rm tis}) M_{\rm tis} \ , \tag{25}$$

where $M_{\rm tis}$ is the PFT-dependent tissue-mortality factor.

Finally, the grid cell average individual tissue carbon after fire is updated as

$$C_{{\rm tis},i,{\rm new}} = \frac{(1-k_{\rm fire}) + k_{\rm fire}(1-\xi)(1-L_{\rm tis})(1-M_{\rm tis})}{1-k_{\rm fire}\xi} C_{{\rm tis},i} \ , \tag{26}$$

where the denominator gives the percentage of individuals that survive after the fire (within the whole grid cell); the first term of the numerator is the percentage of individuals outside the fire burn-area (whose carbon pools remain unchanged); and the second term accounts for the proportion of tissue remaining, belonging to individuals that have survived, inside the burn–area, and the term $C_{{\rm tis},i}$ on the right hand side is the individual tissue carbon before fire.

To offer an interface with atmospheric chemistry and aerosol models in ESMs, the fire model also estimates trace gas and aerosol emissions, $E_{x,i}$ (g species per unit area of grid cell), following Andreae and Merlet (2001) as

$$E_{x,i} = F_{x,i} k_{\rm fire} P_i \frac{\Delta C_{{\rm fire,tis},i}}{[C]} \ , \tag{27}$$

where x is the index of trace gas and aerosol; $F_{x,i}$ [g species (kg dm)$^{-1}$] is the PFT-dependent emission factor; and $[C] =$ 450 gC (kg dm)$^{-1}$ is a conversion factor from tissue dry matter to carbon.

2.6. *Ecosystem large-scale properties*

Important ecosystem large-scale properties, e.g., LAI and FC, are updated depending on the related state variables.

2.6.1. *Leaf area index*

Leaf area index of a specific PFT is defined as total leaf area per unit land area covered by the PFT. For woody PFTs, it is calculated as

$${\rm LAI}_i = \frac{C_{l,i}{\rm SIA}}{a_{{\rm C},i}} \ , \tag{28}$$

where $C_{{\rm l},i}$ and $a_{C,i}$ are the individual crown area and leaf carbon, respectively.

Because grass has no pre-defined morphology, and is assumed to always have a population density of one individual per area of grid cell, we virtually define its crown area, following some empirical approximation, as

$$a_{{\rm C},i} = 1 - e^{-0.5 C_{1,i}{\rm SLA}} \ , \tag{29}$$

so that the LAI of grass can be calculated using Eq. (28) and is similar to the definition in other DGVMs.

2.6.2. *Fractional coverage*

To be consistent with the definition commonly used in LSMs, in IAP-DGVM the fractional coverage of a specific PFT is the percentage of grid cell area that is covered by the crown area of that PFT, calculated as

$${\rm FC}_i = a_{{\rm C},i} P_i \ . \tag{30}$$

For woody PFTs, CA is calculated in allocation (section 2.3), and P is updated in the population dynamics part. For grass

PFTs, CA is calculated using Eq. (29) (section 2.6.1), and $P \equiv 1$. Note that this is different to the concept of fractional projective cover adopted in some DGVMs, e.g., LPJ [Eq. (8) of Sitch et al. (2003)] and CLM-DGVM [Eq. (28) of (Levis et al., 2004)].

3. Demonstration of model performance

3.1. *Simulation setup*

To demonstrate the model performance, IAP-DGVM was coupled to the Community Land Model (CLM3.0), and a global offline simulation at T-62 resolution (192×79 grid cells covering 180°W–180°E, 60°S–90°N) was performed. The near-surface atmospheric data of Qian et al. (2006) for the period 1950–99 were used as the forcing data, which include temperature, humidity, wind, precipitation, downward solar radiation, and surface pressure.

The simulation started with all grid cells as bare ground, without pre-established vegetation. In order for ecosystems in most regions—in particular the boreal regions—to approach their equilibrium states, an 800-yr simulation was performed, driven by the cycling of available forcing data. The first 750 years of the simulation was treated as the spin-up period, and the results from the last 50 years were averaged over each grid cell.

Two datasets of observed global vegetation distribution were used to evaluate the model performance: (1) The CLM4 surface vegetation dataset, which is derived from MODIS observations, incorporating the cropping information from Ramankutty et al. (2008), and is designed to provide land surface vegetation information (e.g., FC, height of canopy top, monthly LAI of different PFTs) to be used in land surface model simulations; (2) The Harmonized World Soil Database (HWSD), which was developed from an interim report of the International Institute for Applied Systems Analysis (IIASA). The HWSD Supplementary Data of Land Use and Land Cover is a compilation of an inventory of seven major land cover/land use categories, i.e., forest, grass/scrub/woodland, barren and very sparsely vegetated land, urban and built-up land, water, rain-fed cultivated land, and irrigated cultivated land.

3.2. *Global vegetation distribution*

The PFT FCs over the last 50 years of the simulation were averaged and then summed into four categories, i.e., tree (7 PFTs); shrub (2 PFTs); grass (3 PFTs); and bare soil. Because IAP-DGVM does not simulate cropland, in order to reduce the influence of the absence of cropland in the evaluation, the vegetation coverage in each grid cell was multiplied by a factor of $(100\% - \mathrm{FC_{crop}})$, where $\mathrm{FC_{crop}}$ is the fraction of crop coverage in the CLM surface dataset.

Figure 2 shows the simulated global vegetation distribution against observation. As can be seen, IAP-DGVM is able to correctly reproduce the two major forest zones, i.e., the tropical rainforest zone over the Amazon, central Africa, and southern Asia (e.g., Indonesia), and the boreal forest zone over the northern part of Eurasia and North America. Besides, it also reproduces the temperate forest over southeast China. However, it overestimates the global forest coverage as 44.8×10^6 km^2, compared with 37.5×10^6 km^2 and 37.7×10^6 km^2 derived from CLM4 and HSWD data, respectively, mainly by overestimating the central forest area (i.e., the region with tree coverage over 70%). On the other hand, it underestimates the peripheral forest area (i.e., tree coverage under 30%).

Shrubland is mainly seen in the far north regions of Asia and North America, in good agreement with the CLM4 dataset. Temperate shrubland is distributed in large areas over the subtropical arid to semiarid regions in southwestern North America, Australia, the Middle East, southern Africa, and northern China, but the FC is usually below 60%.

Grassland appears across the vast majority of the global land surface, except in most arid regions. However, the model shows less grass coverage compared with CLM4 (20.3×10^6 km^2 v.s. 26.0×10^6 km^2). It reproduces the center regime of grassland in central and southern Africa as well as the central United States, but misses the temperate grasslands of Asia and eastern South America. On the other hand, the grassland area produced in the center of North Asia is not shown in CLM4 observations. This implies that the parameterization of grass in IAP-DGVM needs further improvement.

In terms of desert, the model results show these areas to be mainly distributed in the Sahara, Middle East, northwest of China and North America, and Australia, which is in good agreement with observations.

Figure 2 also shows that there is a difference between the two observational datasets. Although they have similar forest coverage, the HSWD dataset has a larger total coverage of shrub- and grassland (46.4×10^6 km^2) than CLM4 (39.1×10^6 km^2), as well as the IAP-DGVM simulation (34.9×10^6 km^2), and a smaller bare soil coverage (34.9×10^6 km^2) than CLM4 (42.4×10^6 km^2) and IAP-DGVM (39.3×10^6 km^2).

Figure 3 shows the global dominant vegetation types. A grid cell is classified as desert if the bare soil coverage is greater than 50%; otherwise, it is classified as the PFT with the highest FC. The results from IAP-DGVM were compared with the CLM4 dataset only, because the HSWD dataset does not provide information on PFTs. As can be seen, the model reproduces the transition from forest to grassland (savanna) in the tropical region, and from forest to shrubland in the boreal region. However, it overestimates the region of temperate forest replacing grassland in eastern Asia and North America, and incorrectly presents temperate forest replacing boreal forest in the northern part, and grassland in the southern part of Europe. Besides, distinguishing between desert and temperate shrubland is also difficult in the model.

4. Discussion and conclusions

IAP-DGVM considers vegetation processes at various scales, including biogeophysics and biogeochemistry, individual and population dynamics, and biogeography, as well

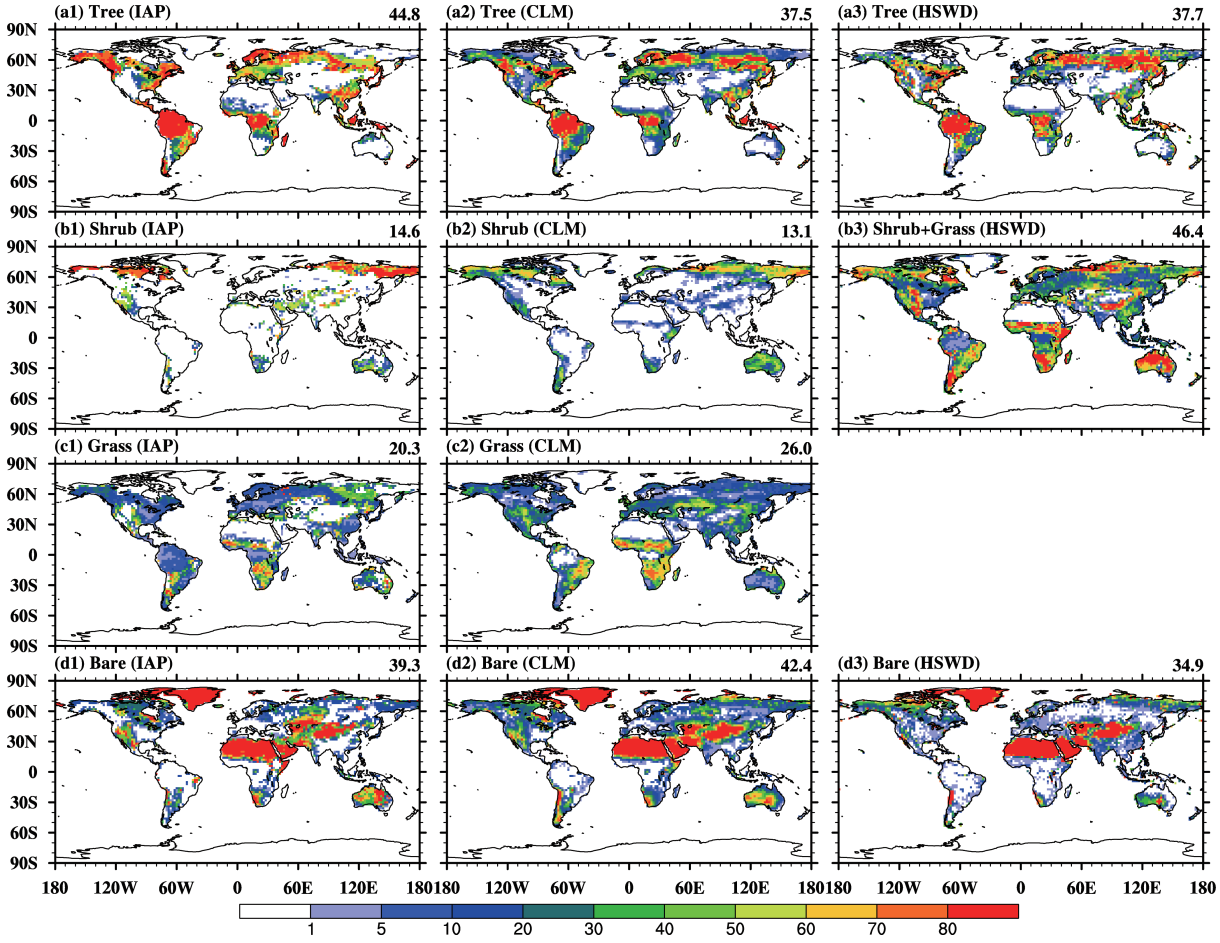

Fig. 2. Global distribution of the percentage coverage of (a1) trees, (b1) shrub, (c1) grass, and (d1) bare soil simulated by IAP-DGVM. The observed distribution from the CLM4 surface dataset (a2–d2) and HSWD (a3–d3) are also shown for comparison. The number in the top-right corner shows the global coverage (over 60°S–90°N, 180°W–180°E) in 10^6 km^2 of the corresponding category.

as environmental disturbance due to fire. With a specifically designed shrub sub-model, IAP-DGVM can correctly reproduce the global distribution of temperate and boreal shrubland, which is missing in several other DGVMs (e.g., Moorcroft et al., 2001; Sitch et al., 2003; Levis et al., 2004), where it is unrealistically replaced by grass and bare soil. However, while the model can distinguish shrubland from forest in boreal regions, the competition among temperate shrub, grass and bare soil in the arid to semiarid regions becomes more complex, and so it is more difficult to accurately predict the dominant vegetation type there.

IAP-DGVM adopts the process-based fire parameterization of Li et al. (2012a, 2012b), which considers the impacts of both natural and anthropogenic activities on fire occurrence and propagation This fire parameterization scheme has been tested on other ecosystem model platforms and the simulations of burned area, fire seasonality, fire interannual variability, and fire carbon emissions are in close agreement with observations (Li et al., 2012a, 2012b, 2013). Furthermore, it has the capability to simulate trace gas and aerosol emissions due to biomass burning (Li et al., 2012a, 2012b), providing an interface for coupling with atmospheric chemistry and aerosol models in ESMs. The impacts of fire on ecosystem distribution and structure are being evaluated.

The essential role of DGVMs in ESMs is to simulate the dynamics of vegetation distribution and structure, including ecosystem equilibrium states, vegetation interannual variation under climate perturbation, and ecosystem transition along with climate change. In this paper, together with the results shown from other DGVMs (e.g., Sitch et al., 2003; Bonan and Levis, 2006; Zeng, 2010), we have demonstrated that DGVMs are capable to capture the major regions of each vegetation category (i.e., tree, shrub, grass, and bare soil) under current climate conditions, as well as vegetation–climate relationships. However, besides the differences and uncertainties among current DGVMs (Sitch et al., 2008), there are some common biases. For example, Fig. 2 shows that the model overestimates areas with higher tree or shrub coverage, but underestimates peripheral areas. As a consequence, most current DGVMs find it difficult to reproduce the transition zones between different ecosystems (i.e., ecotones), where vegetation is fragile to climate and environment changes. Besides, DGVMs tend to produce ecosystems with single dominant PFTs and vegetation classes (e.g., Hughes et al., 2004),

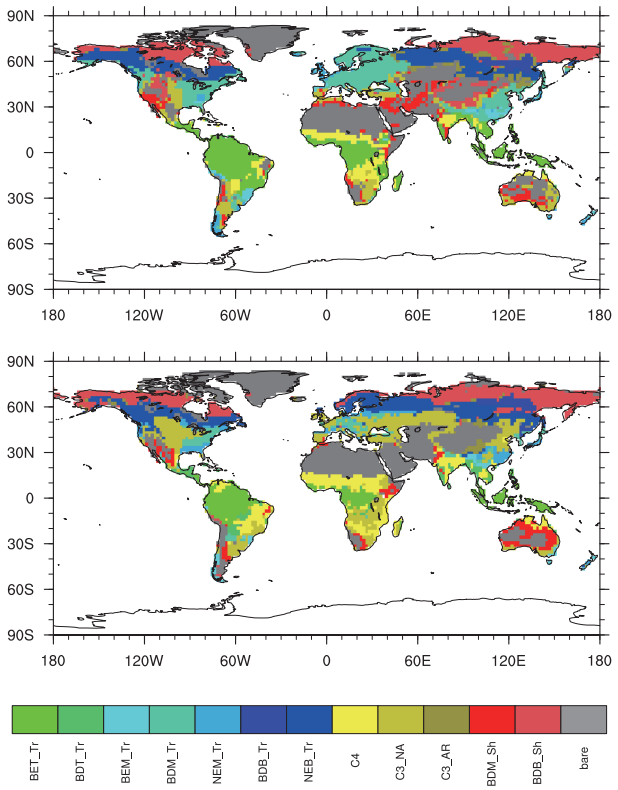

Fig. 3. Global distribution of dominant vegetation types obtained from (a) IAP-DGVM and (b) CLM4.

and hence underestimate biodiversity.

Some DGVMs, including IAP-DGVM, apply the mean field theory approximation, representing woody PFTs with a population of average individuals. Such simplification may dramatically reduce the computational complexity while still conserving large-scale ecosystem states (e.g., FC and LAI). However, neglecting individual differences leads to some systematic bias in the simulated ecosystem structure. In another study, we showed that the revised CLM-DGVM predicts unrealistically high population density with small individual sizes of tree PFTs in boreal forests (Song et al., 2013), and hence underestimates ecosystem biomass. In IAP-DGVM, the percentage of small individual trees is reduced (data not shown), but the above bias still exists. Further improvements of the model may involve the introduction of spatial heterogeneities from both the biotic (plant age, size and traits) and abiotic (microclimatic) aspects.

Acknowledgements. This work was supported by the Chinese Academy of Sciences Strategic Priority Research Program (Grant No. XDA05110103) and the State Key Project for Basic Research Program of China (Grant No. 2010CB951801).

REFERENCES

Andreae, M. O., and P. Merlet, 2001: Emission of trace gases and aerosols from biomass burning. *Global Biogeochemical Cycles*, **15**, 955–966.

Bonan, G. B., and S. Levis, 2006: Evaluating aspects of the Community Land and Atmosphere Models (CLM3 and CAM3) using a dynamic global vegetation model. *J. Climate*, **19**, 2290–2301.

Bowman, D. M. J. S., and Coauthors, 2009: Fire in the Earth system, *Science*, **324**, 481–484, doi: 10.1126/science.1163886.

Box, E. O. 1981: *Macroclimate and Plant Forms: An Introduction to Predictive Modeling in Phytogeography.* Vol. 1, *Tasks for Vegetation Science*, Springer, 258 pp.

Bugmann, H., 2001: A review of forest gap models. *Climatic Change*, **51**, 259–305.

Cox, P. M., 2001: Description of the TRIFFID Dynamic Global Vegetation Model. Hadley Centre Tech. Note 24, Hadley Centre, Bracknell, U.K., 16 pp.

Davidson, E. A., and Coauthors, 2012: The Amazon basin in transition. *Nature*, **481**, 321–328.

Foley, J. A., I. C. Prentice, N. Ramankutty, S. Levis, D. Pollard, S. Sitch, and A. Haxeltine, 1996: An integrated biosphere model of land surface processes, terrestrial carbon balance, and vegetation dynamics. *Global Biogeochemical Cycles*, **10**, 603-628.

Friend, A. D. , A. K. Stevens, R. G. Knox, and M. G. R. Cannell, 1997: A process-based, terrestrial biosphere model of ecosystem dynamics (Hybrid v3.0). *Ecological Modelling*, **95**, 249-287.

Hughes, J. K., P. J. Valdes, and R. A. Betts, 2004: Dynamical properties of the TRIFFID dynamic global vegetation model. Hadley Centre Tech. Note 56, Hadley Centre, Bracknell, U.K., 23 pp.

Keane, R. E., M. Austin, C. Field, A. Huth, M. J. Lexer, D. Peters, A. Solomon, and P. Wyckoff, 2001: Tree mortality in gap models: application to climate change. *Climatic Change*, **51**, 509–540.

Lenton, T. M., 2011: Early warning of climate tipping points. *Nature Climate Change*, **1**, 201–209.

Lenton, T. M., H. Held, E. Kriegler, J. W. Hall, W. Lucht, S. Rahmstorf, and H. J. Schellnhuber, 2008: Tipping elements in the Earth's climate system. *Proc. Natl. Acad. Sci., USA*, **105**, 1786–1793.

Levis, S., G. B., Bonan, M. Vertenstein, and K. W. Oleson, 2004: The Community Land Model's dynamic global vegetation model (CLM-DGVM): Technical description and user's guide NCAR Tech. Note TN-459+IA, National Center for Atmospheric Research, Boulder, 50 pp.

Li, F., X. D. Zeng, and S. Levis, 2012a: A process-based fire parameterization of intermediate complexity in a Dynamic Global Vegetation Model. *Biogeosciences*, **9**, 2761–2780.

Li, F., X. D. Zeng, and S. Levis, 2012b: Corrigendum to "A process-based fire parameterization of intermediate complexity in a Dynamic Global Vegetation Model" published in Biogeosciences, 9, 2761–2780, 2012. *Biogeosciences*, **9**, 4771–4772, doi: 10.5194/bg-9-4771-2012.

Li, F., S. Levis, and D. S. Ward, 2013: Quantifying the role of fire in the Earth system–Part 1: Improved global fire modeling in the Community Earth System Model (CESM1). *Biogeosciences*, **10**, 2293–2314.

Lugo, A. E., S. L. Brown, R. Dodson, T. S. Smith, and H. H. Shugart, 1999: The Holdridge Life Zones of the conterminous United States in relation to ecosystem mapping. *Journal of Biogeography*, **26**, 1025–1038.

Moorcroft, P. R., G. C. Hurtt, and S.W. Pacala, 2001: A method for scaling vegetation dynamics: The ecosystem demography

model (ED). *Ecol. Monogr.*, **71**, 557–586.

Nobre, C. A., and L. S. Borma, 2009: 'Tipping points' for the Amazon forest. *Current Opinion in Environmental Sustainability*, **1**, 28–36, doi: 10.1016/j.cosust.2009.07.003.

Potter, C. S. and S. A. Klooster, 1999: Detecting a terrestrial biosphere sink for carbon dioxide: Interannual ecosystem modeling for the mid-1980s. *Climatic Change*, **42**, 489-503.

Prentice, I. C., M. T. Sykes, and W. Cramer, 1993: A simulation model for the transient effects of climate change on forest landscapes. *Ecological Modelling*, **65**, 51–70.

Prentice, I. C., A. Bondeau, and Coauthors, 2007: Dynamic Global Vegetation Modeling: Quantifying Terrestrial Ecosystem Responses to Large-Scale Environmental Change. *Terrestrial Ecosystems in a Changing World*, J. G. Canadell, Ed., The IGBP Series, Springer-Verlag, 175–192.

Qian, T. T., A. G. Dai, K. E. Trenberth, and K. W. Oleson, 2006: Simulation of global land surface conditions from 1948 to 2004. Part I: Forcing data and evaluations. *Journal of Hydrometeorology*, **7**, 953–975.

Ramankutty, N., A. T. Evan, C. Monfreda, and J. A. Foley, 2008: Farming the planet: 1. Geographic distribution of global agricultural lands in the year 2000. *Global Biogeochemical Cycles*, **22**, GB1003, doi: 10.1029/2007GB002952.

Ricklefs, R. E.,2008: *The Economy of Nature*. 6th ed. W H Freeman & Co., 550 pp.

Sato, H., A. Itoh, and T. Kohyama, 2007: SEIB-DGVM: A new dynamic global vegetation model using a spatially explicit individual-based approach. *Ecological Modelling*, **200**, 279–307, doi: 10.1016/j.ecolmodel.2006.09.006

Scheffer, M., S. Carpenter, J. A. Foley, C. Folke, and B. Walker, 2001: Catastrophic shifts in ecosystems. *Nature*, **413**, 591–596.

Scheffer, M., and Coauthors, 2009: Early-warning signals for critical transitions. *Nature*, **461**, 53–59.

Sitch, S., and Coauthors, 2003: Evaluation of ecosystem dynamics, plant geography and terrestrial carbon cycling in the LPJ dynamic global vegetation model. *Global Change Biology*, **9**, 161–185.

Sitch, S., and Coauthors, 2008: Evaluation of the terrestrial carbon cycle, future plant geography and climate-carbon cycle feedbacks using five Dynamic Global Vegetation Models (DGVMs). *Global Change Biology*, **14**, 2015–2039, doi: 10.1111/j.1365-2486.2008.01626.x

Song, X., 2012: The research on population dynamics in Dynamic Global Vegetation Model. Ph.D. dissertation, Institute of Atmospheric Physics, Chinese Academy of Science, 102 pp. (in Chinese)

Song, X. and X. D. Zeng, 2014: Investigation of uncertainties of establishment schemes in Dynamic Global Vegetation Models. *Adv. Atmos. Sci.*, **31**, 85–94, doi: 10.1007/s00376-013-3031-1.

Song, X., X. D. Zeng, and J. W. Zhu, 2013: Evaluating the tree population density and its impacts in CLM-DGVM. *Adv. Atmos. Sci.*, **30**, 116–124, doi: 10.1007/s00376-012-1271-0.

Woodward, F. I., M. R. Lomas, and S. E. Lee, 2000: Predicting the future production and distribution of global terrestrial vegetation. *Terrestrial Global Productivity*, J. Roy, Ed, Academic Press, 519–539.

Zeng, X. D., 2010: Evaluating the dependence of vegetation on climate in an improved dynamic global vegetation model. *Adv. Atmos. Sci.*, **27**, 977–991, doi: 10.1007/s00376-009-9186-0.

Zeng, X. D., X. B. Zeng, and M. Barlage 2008: Growing temperate shrubs over arid and semiarid regions in the Community Land Model–Dynamic Global Vegetation Model. *Global Biogeochemicla Cycles*, **22**, doi: 10.1029/2007GB003014.